Korean J. Chem. Eng., 38(9), 1946-1955 (2021)
DOI: 10.1007/s11814-021-0848-7

pISSN: 0256-1115
eISSN: 1975-7220

Thermal properties and curing kinetics of epoxy powder coatings containing graphene nanoplatelets

Andrielen Braz Vanzetto*,†, Lucas Dall Agnol, Alessandra Lavoratti*, Marcos Vinícius Marocco***, Gabriel Gonem de Lima***, Lilian Vanessa Rossa Beltrami*, Ademir José Zattera*, and Diego Piazza***

*Postgraduate Program in Process and Technology Engineering (PGEPROTEC), University of Caxias do Sul (UCS), Caxias do Sul, RS - Brazil
**Postgraduate Program in Materials Science and Engineering (PGMAT), University of Caxias do Sul (UCS), Caxias do Sul, RS - Brazil
***Laboratory of Polymers (LPOL), University of Caxias do Sul (UCS), 1190 Francisco Getúlio Vargas St. Caxias do Sul, RS - Brazil
(*Received 30 August 2020 • Revised 14 April 2021 • Accepted 18 May 2021*)

Abstract−Graphene nanoplatelets (GNP) have excellent properties, such as high mechanical strength and good thermal conductivity, making them interesting nanofiller for their application in powder coatings. In this context, the aim of this study was to evaluate the thermal behavior and the curing kinetics of epoxy powder coatings containing GNP. The coatings were obtained by mixing in a ball mill followed by homogenization in molten state. The GNP were dispersed directly into the epoxy powder. The morphology, thermal stability and curing kinetics of the samples were evaluated. During the curing process, the GNP accelerated the onset of the reaction but ultimately caused steric impediment. From the results, the GNP incorporated to the solid epoxy resin for coatings behaved differently in each stage of the curing process. In general, while the direct dispersion of GNP in powder epoxy by dry mixing methods was not ideal, the thermal properties were improved, with GNP inducing a poor curing state where diffusion phenomena are predominant.

Keywords: Epoxy Powder Coatings, Graphene Nanoplatelets, Curing Kinetics, Thermal Properties

INTRODUCTION

Graphene nanoplatelets (GNP) have emerged as a promising class of carbon nanofillers to improve the performance of epoxy coatings. Not only are they cost effective, but also well compatible with most polymers, high aspect ratio and high specific strength [1]. GNP are three-dimensional particles formed by stacked two-dimensional layers of graphene, where one of the external dimensions is at nanoscale [2]. GNPs are useful for improving the physical properties of polymers and for producing multifunctional polymer composites that can be used in a wide range of applications [3,4].

The processing of GNP nanocomposites and coatings has some difficulties associated with the effective dispersion of these nanofillers in polymer matrices, because of the strong tendency of GNP to form agglomerates [5,6]. This is mainly due to the strong interactions between graphene layers, making the percolation of resin molecules into the layers difficult [7]. As such, the properties of graphene-based composites are strongly governed by the state of dispersion and the degree of exfoliation of the nanoplatelets [8,9]. The incorporation of graphene and its derivatives in coatings usually occurs in liquid media, with most studies using solvents such as acetone and alcohol as a processing aid. However, powder coatings are a different system, and the literature data about the dispersion of graphene materials in dry coatings is still recent.

According to Gorrasi et al. [10], mixing methods in solid state such as mixing by spherical grinding, proved to be an alternative to achieve a good dispersion of nanoparticles in polymers while avoiding working at high temperatures and/or with solvents. The addition of a solvent to aid the dispersion and the exfoliation of graphene in powder coatings is a common theme. On the other hand, the use of an extra solvent goes against the principle of the environmental friendliness of the powder coatings.

The formation of reticulated networks in thermoset materials depends on the ease of the curing progress in the different stages of the reaction. The cure of thermoset systems is a complex process involving reactions between monomers or oligomers and a cross-linking agent. Monitoring the evolution of the cure reactions allows one to determine the thermodynamic and kinetic parameters, such as heat (enthalpy) and activation energy of the curing reaction, glass transition temperature, speed constant, reaction order and curing reaction speed, all of which are important data to define processing conditions. In this context, the study of the curing behavior and kinetics provides useful information about the characteristics of the final product [7,11]. According to Ferdosian et al. [12], chemical reactions during curing are accompanied by complex physical phenomena. These reactions would be even more complicated when solid epoxy is used, specifically in the presence of nanoparticles.

Many different analytical methods for characterizing the curing reaction and monitoring the thermoset curing process have been studied. Among them, differential exploratory calorimetry (DSC) has

†To whom correspondence should be addressed.
E-mail: andrielenvanzetto@gmail.com

been cited as a reliable analysis. This method can provide information on the glass transition temperature (T_g), onset of the curing process, heat of reaction, maximum curing rate, completion of cure and degree of cure [13,14].

Jouyandeh et al. [15] studied the curing kinetics of epoxy/graphene oxide system using isoconversional methods based on DSC analyses to evaluate the activation energy of the systems as a function of the extent of reaction. The authors concluded that the addition of graphene oxide promoted the increase of the activation energy in comparison to the neat epoxy. Nonahal et al. [7] also studied the curing kinetics of epoxy coatings containing graphene oxide by means of DSC. The authors observed that the curing mechanism remained unchanged after the introduction of the nanoparticles, despite considerable changes in the network formation and in the final properties.

Although other graphene nanomaterials have been studied regarding their influence on the curing kinetics of the epoxy resin, the use of GNP in powder coatings is a recent trend. In this context, the aim of this work is to incorporate GNP in epoxy powder coatings by means of dry mixing, and to evaluate the influence of GNP addition on the thermal properties and curing kinetics of the coatings.

EXPERIMENTAL

1. Materials

A bisphenol-A epoxy resin (ARALDITE GT 7004 ES) was used in solid form, with a softening point of 85-95 °C, supplied by PVT Tintas (RS, Brazil). The curing agent was 1-o-tolylbiguanide ($C_9H_{13}N_5$), derived from dicyandiamide (CASIMID 710 OILED PR9990), with a melting point of 140 °C. The spreading agent used was Resiflow TM PV-60. A surface agent benzoin (2-hydroxy-1,2-diphenylethanone), with a melting point of 132-135 °C, was supplied by PVT Tintas (Brazil). Graphene nanoplatelets (CAS 1034343-98-0) were obtained from Strem Chemicals (USA) with a thickness 6-8 nm and a width of 5 μm, with a surface area of 120 $m^2 \cdot g^{-1}$. The carbon, oxygen and residual acid content supplied by the manufacturer were 99.5%, 1% and 0.5%, respectively. All materials and chemical reagents were used as received without further purification.

2. Preparation of the Coatings

Three epoxy powder coating formulations were prepared containing 0, 1 and 2 wt% per weight of GNP, named 0GNP, 1GNP and 2GNP, respectively. In all formulations, 5 wt% curing agent, 1 wt% spreading agent and 0.5 wt% benzoin were added. The concentration of GNP was chosen based on literature results [16-18].

The epoxy resin and the GNP were prehomogenized in a stainless-steel ball mill (DeLeo brand, model DL-MB), with 30 mm diameter alumina spheres, for 30 minutes at a constant speed of 50 rpm. Subsequently, the materials were mixed in molten state in a co-rotating twin screw extruder, model MH-COR-LAB (MH Equipamentos Ltda., Brazil) with L/D 44, 20 mm thread diameter, operating at a speed of 200 rpm with a temperature profile ranging from 60 °C to 90 °C. After extrusion, the samples were cooled and leveled with the aid of a metallic cylinder. The chips were manually comminuted in a bench knife mill to a 75 μm granulometry to obtain powdered epoxy coatings.

3. Thermal Stability

The thermal stability of the coatings was characterized by thermogravimetric analysis (TGA), in a STA 449 F3 Jupiter® - Netzsch thermogravimetric analyzer, at a temperature range of 25 °C to 800 °C with a heating rate of 10 °C·min^{-1} in nitrogen atmosphere (50 mL·min^{-1}).

4. Curing Kinetics

The curing kinetics of the coatings was monitored by differential scanning calorimetry (DSC) in a Shimadzu DSC-50 equipment, at a temperature range of 25 to 250 °C under a N_2 atmosphere (50 mL·min^{-1}). About 10 mg of sample was analyzed in non-isothermal conditions with four different heating rates of 5, 10, 15 and 20 °C·min^{-1}.

4-1. Kinetic Modelling

The kinetic parameters Eα(T) (activation energy, associated with the energy barrier), *A* (pre-exponential factor, associated with the frequency of vibrations of the activated complex), and f(α) (kinetic function, associated with the reaction mechanism) were determined using the KAS (Kissinger-Akahira-Sunose) method [7]. The kinetic parameters of heterogeneous solid-state reactions are described by Eq. (1):

$$\frac{d\alpha}{dt} = \frac{A}{\beta} e^{\left(-\frac{E_a}{RT}\right)} \cdot f(\alpha) \quad (1)$$

where dα/dt is the reaction rate, A is the pre-exponential factor (min^{-1}), β is the heating rate (dT/dt), Eα is the activation energy (kJ·mol^{-1}), R is the gas constant, T is the absolute temperature (K), f(α) is the hypothetical model function which describes the reaction mechanism, and α is the fractional conversion. In a non-isothermal experiment, α can be calculated by Eq. (2):

$$\alpha = \frac{w_0 - w_t}{w_0 - w_f} \quad (2)$$

where w_0 and w_t are the weight of the sample at t=0 and t=t, respectively, and w_f is the final weight of the sample. From these parameters, the activation energy can be calculated using the KAS method.

The Kissinger-Akahira-Sunose method (KAS) is an integral linear differential with which, by linear regression, the values for the activation energy can be obtained by the resulting slope of ln (β/T^2) vs. 1/T [19]. The KAS method is described by Eq. (3).

$$\ln\left(\frac{\beta}{T^2}\right) = \ln\left(\frac{AR}{E_{a\,KAS} g(\alpha)}\right) - \frac{E_{a\,KAS}}{RT} \quad (3)$$

Lastly, determining the kinetic model f(α) is an important aspect for the prediction of the kinetic behavior of a reaction. All unknown parameters (Eα, A, reaction order, autocatalysis order - for autocatalytic reactions) are found from the fitting of the measured data with the simulated curves for the given reaction types. A statistical comparison of the fits for different models allows the selection of the appropriate model with the corresponding set of parameters. To identify the correct reaction models, different kinetic models commonly found in solid-state reactions were tested from an array of numerical and graphical methods using the Netzsch software [20,21]. The software can analyze a dataset containing rele-

vant dynamic and/or isothermal measurements. Additional information about this software and the tested models can be found at [21].

5. Cure Index

Non-isothermal calorimetry provides useful data to quantify the curing phenomenon in thermoset composites, but there needs to be a universal criterion to generate a unique signature to a thermoset composite cured at a given heating rate. For this, Jouyandeh et al. [11] proposed a dimensionless criterion for typical epoxy-based systems containing nanoparticles. This criterion, called cure index (CI), indicates the effect of the filler concentration on the curing state of thermoset materials. The CI can be calculated from experimental non-isothermal DSC data using the equation proposed by Jouyandeh et al. [11]:

$$CI = \Delta H^{*} \times \Delta T^{*} \quad (4)$$

Where,

$$\Delta H^{*} = \frac{\Delta H_c}{\Delta H_{ref}} \quad (5)$$

$$\Delta T^{*} = \frac{\Delta T_c}{\Delta T_{ref}} \quad (6)$$

And,

$$\Delta T = T_{onset} - T_{endset} \quad (7)$$

T_{onset} and T_{endset} are the initial and final curing temperatures obtained from the DSC curves. ΔH_c and ΔH_{ref} are the values of total heat released during the curing reaction of the thermoset composites and the reference polymer (blank system), respectively. ΔT_c and ΔT_{ref} are, respectively, the curing temperature ranges measured by the equipment for the thermoset composite and the reference polymer.

Jouyandeh et al. [11] defined three possible cases for the state of the cure. If CI is greater than ΔH^{*}, it is assumed that the added filler facilitates curing in relation to the neat polymer, thus being considered a satisfactory cure. If CI is between ΔT^{*} and ΔH^{*} - that is ($\Delta T^{*} < CI < \Delta H^{*}$) - it is assumed that the filler participates efficiently in the cure reaction and is simultaneously intensified by the catalytic and progressive network formations, being considered an excellent cure. And if CI is lower than ΔT^{*}, then the filler behavior is delaying the cure, and so the cure is considered to be poor.

6. Morphology

The morphology of the samples was assessed using field emission gun scanning electron microscopy (FEG-SEM) in a Tescan Mira 3 (Czech Republic) microscope. Before FEG-SEM evaluation, the samples (30 mm×3 mm×1 mm) were cryo-fractured by liquid nitrogen and then were sputter coated with gold using a plasma sputtering apparatus.

RESULTS AND DISCUSSION

1. Thermal Stability

The thermogravimetry (TG) and differential thermogravimetry (DTG) of the coatings are shown in Fig. 1(a)-(b). A weight loss of 80% was detected between 298-422 °C (Fig. 1(a)), associated with

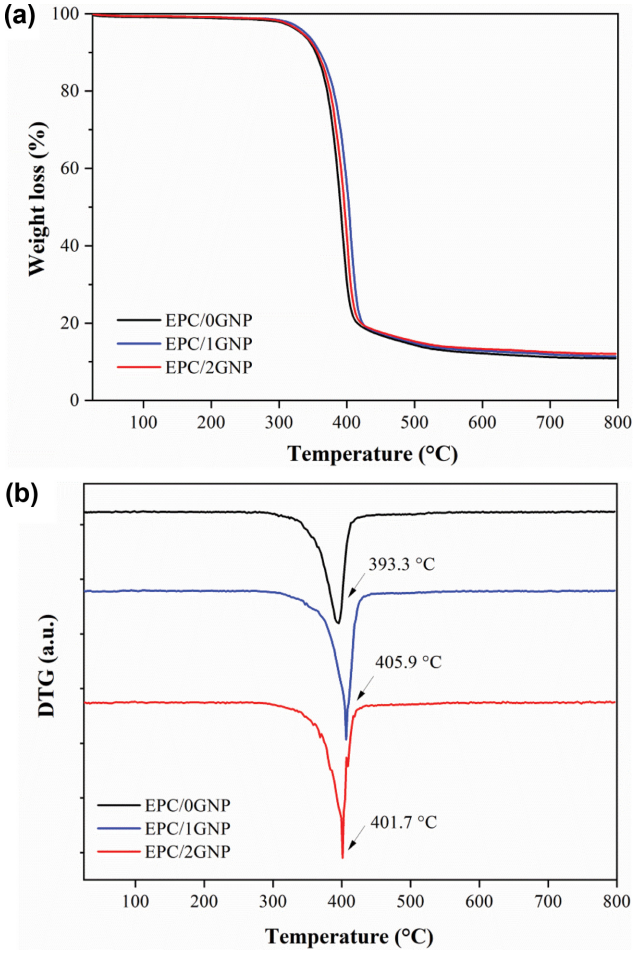

Fig. 1. (a) Thermogravimetry (TG) and (b) differential thermogravimetry (DTG) of pure epoxy-based powder coatings and with 1 and 2 wt% of GNP.

the thermal degradation of the polymeric matrix [16]. From DTG (Fig. 1(b)), the temperature at which the maximum weight loss rate occurred was 393.3 °C for EPC/0GNP, 405.9 °C for EPC/1GNP and 401.7 °C for EPC/2GNP. All samples exhibited a similar degradation profile, suggesting that the existence of GNP did not alter the degradation mechanism of the epoxy matrix [22].

An increase in the maximum degradation temperature was observed for the samples with the addition of GNP in relation to the neat epoxy coating. This increase was 12.6 °C for the EPC/1GNP sample and 8.4 °C for the EPC/2GNP sample. This is attributed to the inherent high thermal stability of graphene nanoplatelets, with a degradation onset of approximately 500 °C per previous studies [23]. Another phenomenon related is that platelet geometry of GNP, when dispersed in a polymer matrix, causes a tortuous-like path effect, which could limit the release of volatile degradation products [16,24].

Above 410 °C, samples containing GNP had a higher solid content compared to the pure epoxy coating. The final residue was 10.9%, 11.4% and 12.1% for the EPC/0GNP, EPC/1GNP and EPC/2GNP samples, respectively. These residues are proportional to the amount of GNP added, due to the high thermal stability of graphene

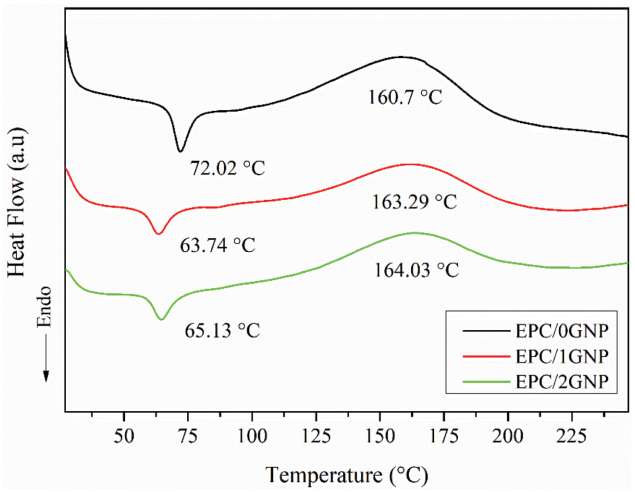

Fig. 2. DSC curves for powder coatings at a heating rate of 10 °C·min^{-1} (first warm-up).

and its derivatives [22,23].

2. Curing Kinetics

Fig. 2 shows the DSC thermograms in the first warm-up run at a rate of 10 °C·min^{-1}. Two main thermal events occur: the first, at 72.02 °C, 63.74 °C and 65.13 °C for the EPC/0GNP, EPC/1GNP and EPC/2GNP samples, respectively, refers to the softening temperature, at which the powder particles melt [25].

There is a decrease in these values with the increase in the content of the GNP, which may be associated with the high thermal conductivity of the GNP, which facilitates the heat transfer between the particles of the powder coating [26].

The second event, related to the curing temperature, occurs between approximately 80 °C and 200 °C, with T_{onset} at 91.9 °C, 85.2 °C and 84.2 °C for samples EPC/0GNP, EPC/1GNP and EPC/2GNP, respectively, and T_{peak} at 160.7 °C, 163.3 °C and 164 °C for EPC/0GNP, EPC/1GNP and EPC/2GNP samples, respectively. There is a significant reduction in the temperature of the onset of curing with the addition of GNP. This observation can be supported by the possible catalytic effect caused by GNP in the epoxy resin curing process [24]. Three major reactions occur during the curing of epoxy resins: a primary-amine epoxy addition, a secondary amine-epoxy addition, and a hydroxyl-epoxy addition (etherification) (Fig. 3). The latter happens when a number of hydroxyl groups are present in either the curing agent or in nanofillers. Previous literature has demonstrated that graphene oxide is able to catalyze the etherification reactions [27]. Since the GNP used in this study has also demonstrated to have a number of hydroxyl-groups [28], albeit in a smaller amount than graphene oxide, and probably derived from their manufacturing process, it is possible that the hydroxyl functionality accelerates the curing process by facilitating the opening of the oxirane ring in the etherification reaction steps.

The maximum curing temperature was not significantly affected by the presence of GNP. However, a reduction in the curing enthalpy values (ΔH_{cure}) was perceived. The enthalpy value of the cure was obtained by integrating the area under the curve of the exothermic event and is associated with the system reactivity. The ΔH_{cure} values found were 67.3 J·g^{-1} for the EPC/0GNP sample, 44.5 J·g^{-1} for the EPC/1GNP sample and 50.7 J·g^{-1} for the EPC/2GNP sample. The reduction in the ΔH_{cure} values in comparison to the neat epoxy coating indicates lower reactivity of the systems containing GNP. The reactions during the curing stage of resins are controlled by the diffusion of the molecules through the network [29]. The presence of lamellar structures can inhibit this movement, leading to a decrease in enthalpy values. This is well documented for clays and may apply to GNP, which is also a lamellar structure. Moreover, epoxy resin units bound to the GNP or situated at the interface may show lower mobility, reducing the conversion of epoxy groups. This has been shown for graphene oxide (GO)/epoxy systems, in which GO contains a high number of hydroxyl groups that participate in the etherification reactions during curing [30]. This behavior was observed for the GNP used in this study on the onset of the curing stage. Albeit with fewer hydroxyl groups, the

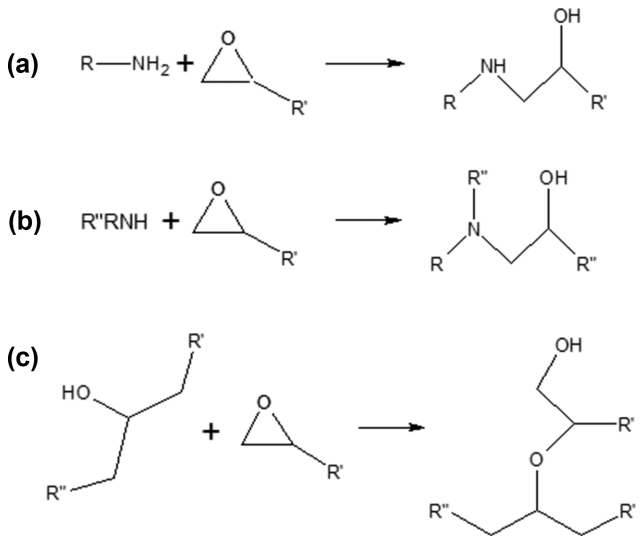

Fig. 3. Major reactions during amine curing of epoxy resins: (a) Primary amine-epoxy addition; (b) secondary amine-epoxy addition; (c) hydroxyl-epoxy addition. Adapted from ref. [27].

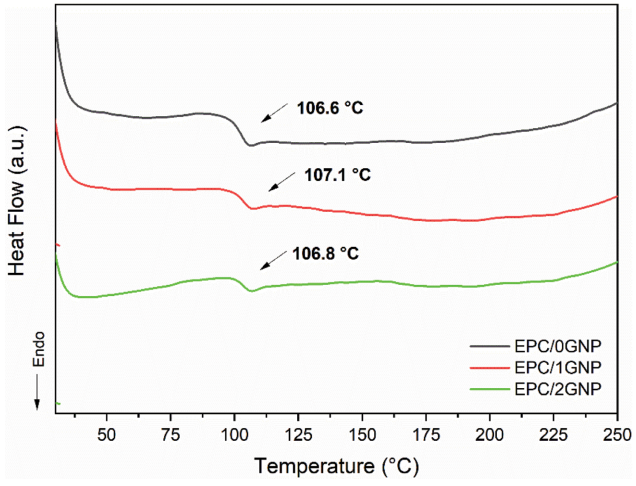

Fig. 4. DSC curves for powder coatings at a heating rate of 10 °C·min^{-1} (second warm-up).

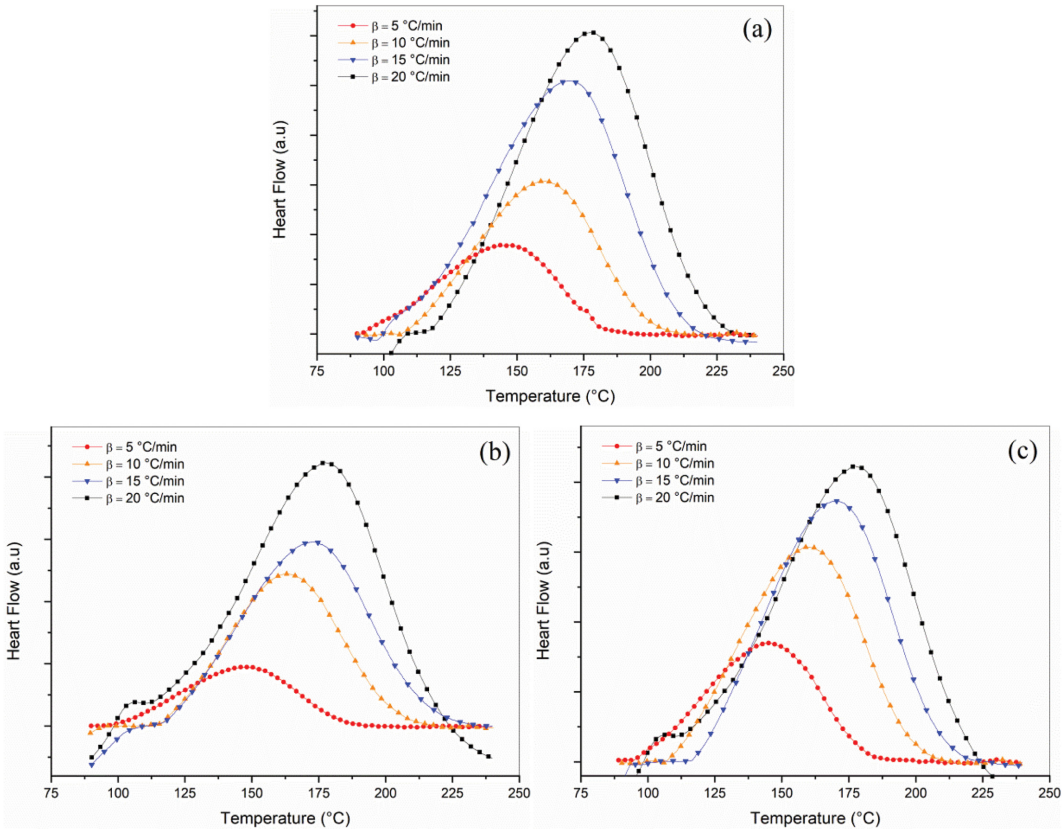

Fig. 5. DSC thermograms of the curing event at the 4 heating rates - (a) EPC/0GNP, (b) EPC/1GNP and (c) EPC/2GNP.

Table 1. Enthalpy values as a function of heating rate

Sample	Enthalpy (J/g)			
	5 °C·min^{-1}	10 °C·min^{-1}	15 °C·min^{-1}	20 °C·min^{-1}
EPC/0GNP	69.15	67.29	65.89	52.81
EPC/1GNP	45.20	44.56	43.29	40.00
EPC/2GNP	54.21	50.74	44.16	40.23

explanation may apply. Lavoratti et al. [28] also reported a decrease in the enthalpy of the cure of epoxy resins containing GNP and attributed this to the formation of agglomerates.

Fig. 4 shows the DSC curves for the samples after curing. A single thermal event was observed at 106.6 °C, 107.1 °C and 106.8 °C for the EPC/0GNP, EPC/1GNP and EPC/2GNP samples, respectively. This event is attributed to the glass transition temperature (T_g), which was not significantly influenced by GNP. No exothermic events were observed, indicating the complete curing of the system.

Fig. 5 shows the DSC curves at four heating rates for all samples, from which the curing kinetics study was carried out. In all cases, it was verified that the maximum heat flow i.e., the peak of each curve, shifts to higher temperatures with increasing heating rate. This is because a slower heating rate offers more time for the chemical reactions of active sites to occur. Likewise, when a shorter time is available for these reactions to occur at higher heating rates, some of the reagents remain unreacted and, therefore, the peaks of the heat flow diagrams are shifted to higher temperatures [7]. The curing enthalpy values (ΔH_{cure}) for each sample at each heating rate are shown in Table 1. The total heat generated during the reaction time is assumed to be directly attributed to the curing reactions. A decrease in enthalpy is observed for samples containing GNP at all heating rates. To explain this phenomenon, one must consider that the lamellar structure of GNP might inhibit the reaction of the reagents and act as a barrier for the release of the energy from the exothermic reaction by the effect of a tortuous path. Thus, the rate of the cure reaction decreases, leading to a lower ΔH value [7]. Prolongo et al. [31] also obtained lower values of ΔH for epoxy/GNP nanocomposites.

The extent of the curing conversion was calculated by Eq. (2). The evolution of the extent of the cure conversion as a function of the temperature calculated for all samples is illustrated in Fig. 6.

In all cases, a sigmoidal pattern was observed, indicating the autocatalytic nature of the curing reaction of the epoxy system [7,32]. The conversion of all samples to a degree of conversion 0.17 occurs

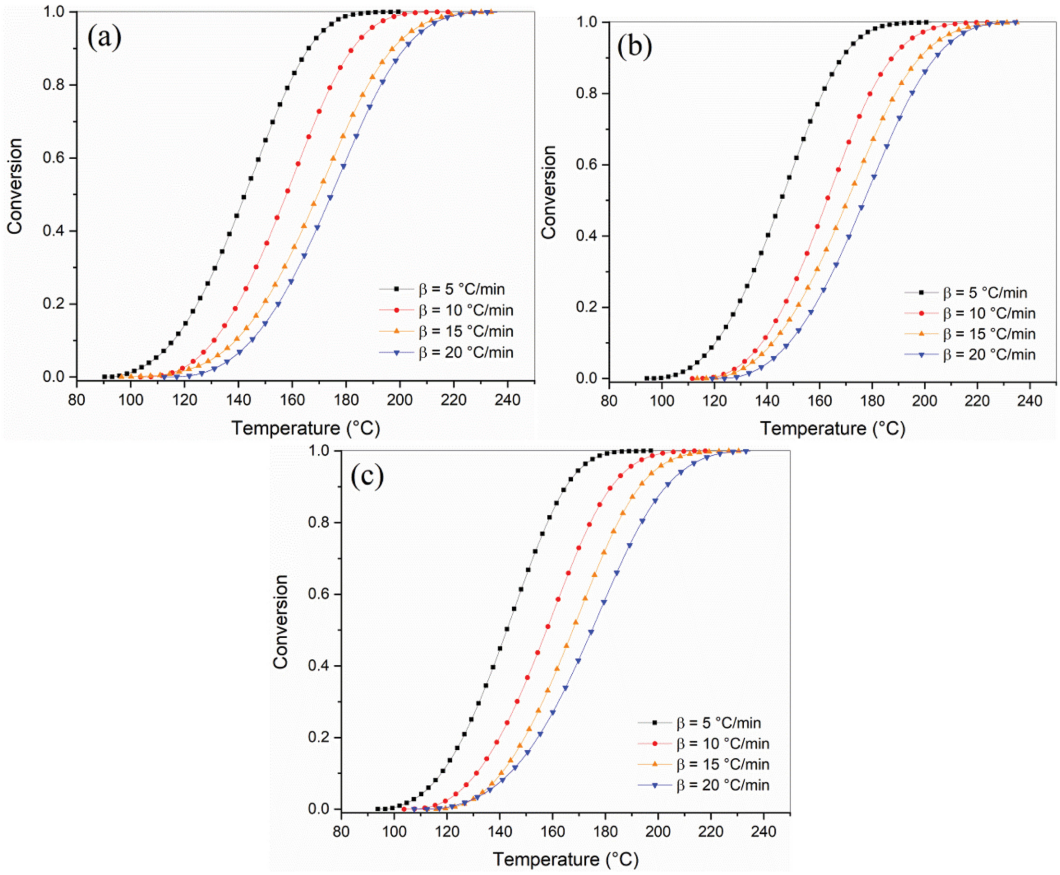

Fig. 6. Degree of conversion versus temperature: (a) EPC/0GNP, (b) EPC/1GNP and (c) EPC/2GNP.

Table 2. Values of the reaction kinetic parameters for neat epoxy and epoxy/GNPs obtained by applying the Bna model

Sample	Ea ($kJ \cdot mol^{-1}$)	Log A (s^{-1})	Reaction order	Exponent a1	Correlation coefficient (r)
EPC/0GNP	65.22	5.769	1.129	0.160	0.996
EPC/1GNP	62.23	5.617	1.198	0.151	0.997
EPC/2GNP	62.37	5.407	1.101	0.145	0.993

at the same temperature. From this degree of conversion, until a degree of conversion 0.98, a delayed effect was observed for samples containing GNP, especially the sample containing 2% GNP. This indicates that at this stage of the reaction, the GNPs make it difficult to form the reticulated network, in line with the results of enthalpy, which indicated less energy release.

The curing reaction as a function of the temperature and the conversion were calculated by Eq. (1), (2), and (3). The linear regression of $\ln(\beta/T_\alpha)$ vs. $1/T_\alpha$ leads to a linear regression, with slope being the activation energy, as seen in Figs. 7 and 8.

The results found so far indicate that there are two concurrent behaviors involved in the curing of epoxy/GNP systems. First, the GNPs act by catalyzing the beginning of the cure as verified by the T_{onset} values observed in DSC results. During the reaction, with the formation of a crosslinked network, they start to act as a physical barrier to the heat transfer. This behavior is reported by Zhi and Huang [24]. The authors clarify that the beginning of the curing process occurs in the liquid state, and therefore the molecules move freely. This fact favors the contact of reactive functional groups, and thus, in this stage, the reaction is controlled kinetically. After the gelation, as the curing process occurs, there is a restriction of the mobility of the reaction system and, in this step, the GNPs interrupt the contact between the reactive groups. Prolongo et al. [31] also report a similar behavior. However, they indicate that this catalytic effect is associated with the high content of GNP incorporation, since they did not report the same phenomenon at low concentrations of filler.

Curing of epoxy resins occurs by autocatalysis [33]. Therefore, the most suitable kinetic model to represent the autocatalytic polymerization reaction was Bna (Expanded Prout-Tompkins equation (na)) [34]. The calculated kinetic parameters by Bna model are shown in Table 2.

The reaction model type and corresponding reaction equation taken from Netzsch thermokinetics software is:

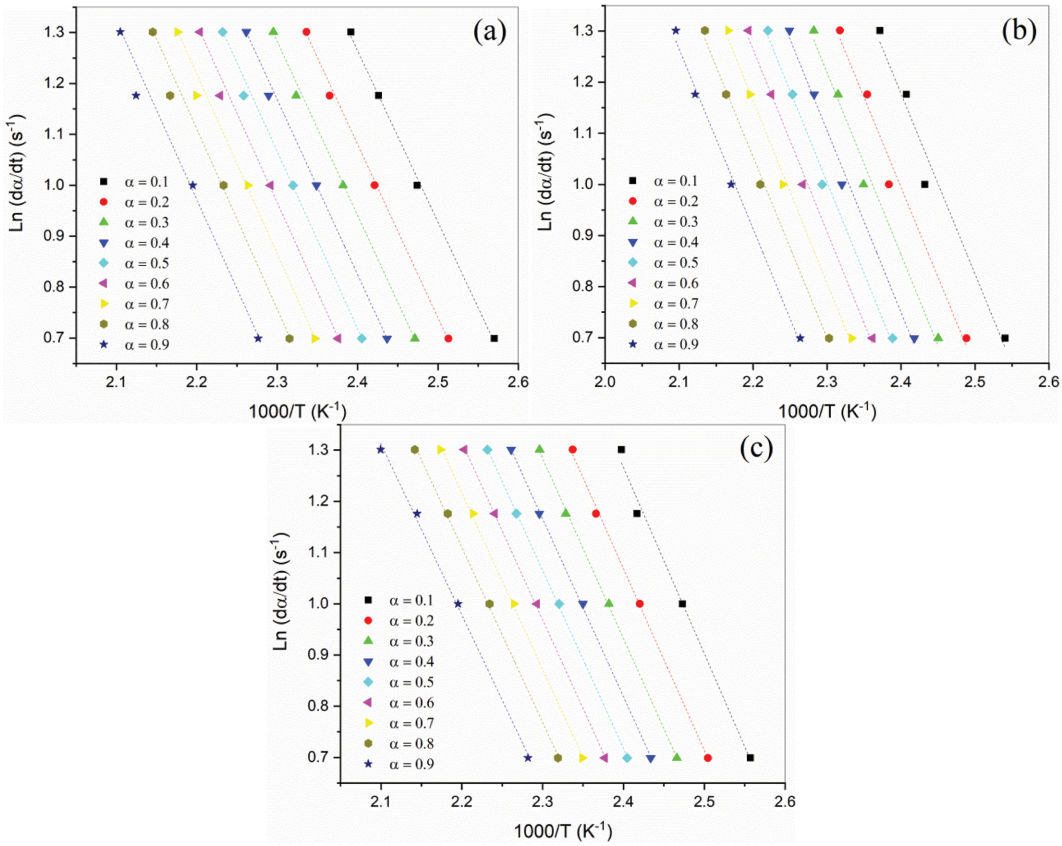

Fig. 7. Plots of ln(dα/dt) *vs.* 1,000/T for (a) EPC/0GNP, (b) EPC/1GNP e (c) EPC/2GNP based on KAS model.

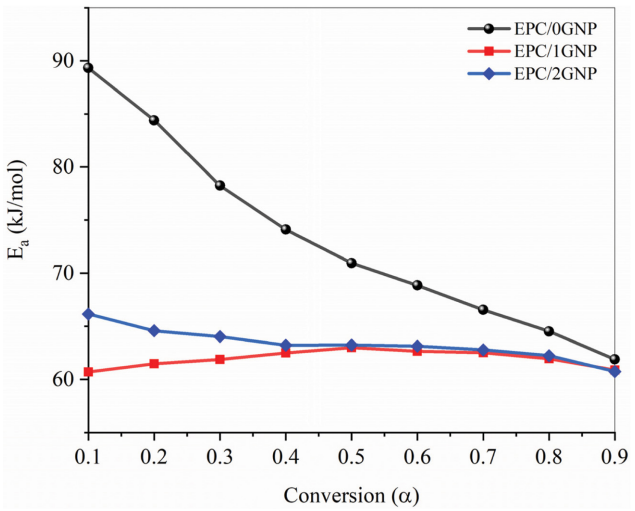

Fig. 8. Dependence of the $E_{\alpha(T)}$ vs. $\alpha_{(T)}$ for neat epoxy and epoxy/GNPs.

$$\frac{de}{dt} = -Ae^{\left(\frac{E}{RT}\right)} f(e, p) \quad (8)$$

where f(e, p) is the expanded Prout–Tompkins equation (Bna). The Bna model is defined by $e^n p^a$. A is the pre-exponential factor; E is the activation energy; R is the gas constant; T is the temperature; a is the conversion degree; e is the starting concentration of the reactant (e=1−α), and p is the concentration of the final product (p=α).

The autocatalytic reaction mechanisms are confirmed by a reaction order value close to 1 found for all samples. A lower mean activation energy is observed for samples containing GNPs in the start of evolution of the cure (Fig. 8), thus indicating that GNPs act as a catalyst in the cure process as discussed earlier.

Performing the comparison between the predicted activation energy results with the experimental data by isoconverison methods is crucial. Fig. 9 shows the experimental data versus the calculated data based on the Bna model. From Fig. 9, we can conclude that the simulations from the Bna model are in good agreement with the experimental conversion calculated at all heating rates for EPC/0GNP, EPC/1GNP and EPC/2GNP.

3. Cure Index

To evaluate the role of GNPs on the curing state of epoxy systems, their cure index was calculated. The results of the cure index calculations are shown in Table 3. There is a variation between the values found for the different heating rates, which is acceptable. However, in general, it can be inferred that CI was lower than ΔT^* for the two concentrations of GNP. As reported by Jouyandeh et al. [11], this result indicates that the curing state of the GNP-containing epoxy system is poor. This phenomenon is observed in thermosetting systems where the filler acts as a steric obstacle in the curing process, which is consistent with the aforementioned results.

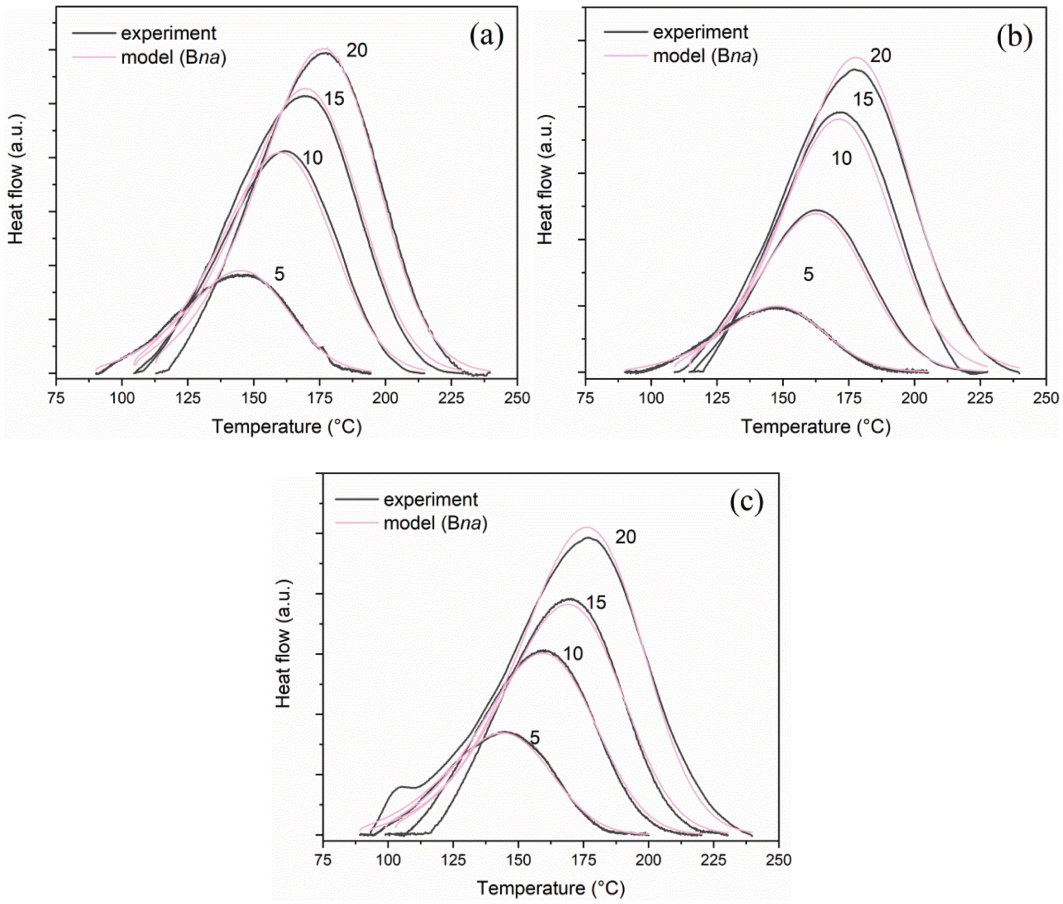

Fig. 9. Model prediction of the polymerization reactions using Prout-Tompkins (Bna) n-th order approach: (a) EPC/0GNP, (b) EPC/1GNP and (c) EPC/2GNP. The different heating rates (in °C/min) at each DSC run are indicated in each curve.

Table 3. Results of the cure index calculations

Sample	CI	ΔH^*	ΔT^*	Ordination	Cure state
EPC/1GNP (5 °C·min^{-1})	0.645	0.654	0.986	CI<ΔT^*	poor
EPC/1GNP (10 °C·min^{-1})	0.545	0.662	0.823	CI<ΔT^*	poor
EPC/1GNP (15 °C·min^{-1})	0.702	0.657	1.068	CI<ΔH^*	good
EPC/1GNP (20 °C·min^{-1})	0.797	0.757	1.052	CI<ΔH^*	good
EPC/2GNP (5 °C·min^{-1})	0.719	0.784	0.917	CI<ΔT^*	poor
EPC/2GNP (10 °C·min^{-1})	0.614	0.754	0.815	CI<ΔT^*	poor
EPC/2GNP (15 °C·min^{-1})	0.696	0.670	1.039	CI<ΔH^*	good
EPC/2GNP (20 °C·min^{-1})	0.806	0.761	1.058	CI<ΔH^*	good

Although in some heating rates the cure status is presented as good (CI>ΔH^*), in all cases the value of ΔH^* was lower than 1, which according to Jouyandeh et al. [15] characterizes a poor cure state, that is, the reaction between cure moieties is hindered by the GNP incorporation, and so the amount of crosslinking is lower than that of the reference system (EPC/0GNP). Jouyandeh et al. [11] highlights two possible cases in this situation:

case a) CI>ΔT^* when T_P^*<1 (9)

case b) CI>ΔT^* when T_P^*<1 (10)

Where,

$$T_P^* = \frac{T_{p,C}}{T_{p,ref}} \quad (11)$$

$T_{p,C}$ and $T_{p,ref}$ are, respectively, the peak temperature of the exothermic reaction of coatings containing GNP and that of the neat epoxy coating, respectively, obtained from the corresponding DSC thermograms. In each case (a or b), a different mechanism is dominant throughout the conversion of the system (diffusion or chemical reaction).

In our results, T_P^* was <1, which, according to Jouyandeh et al.

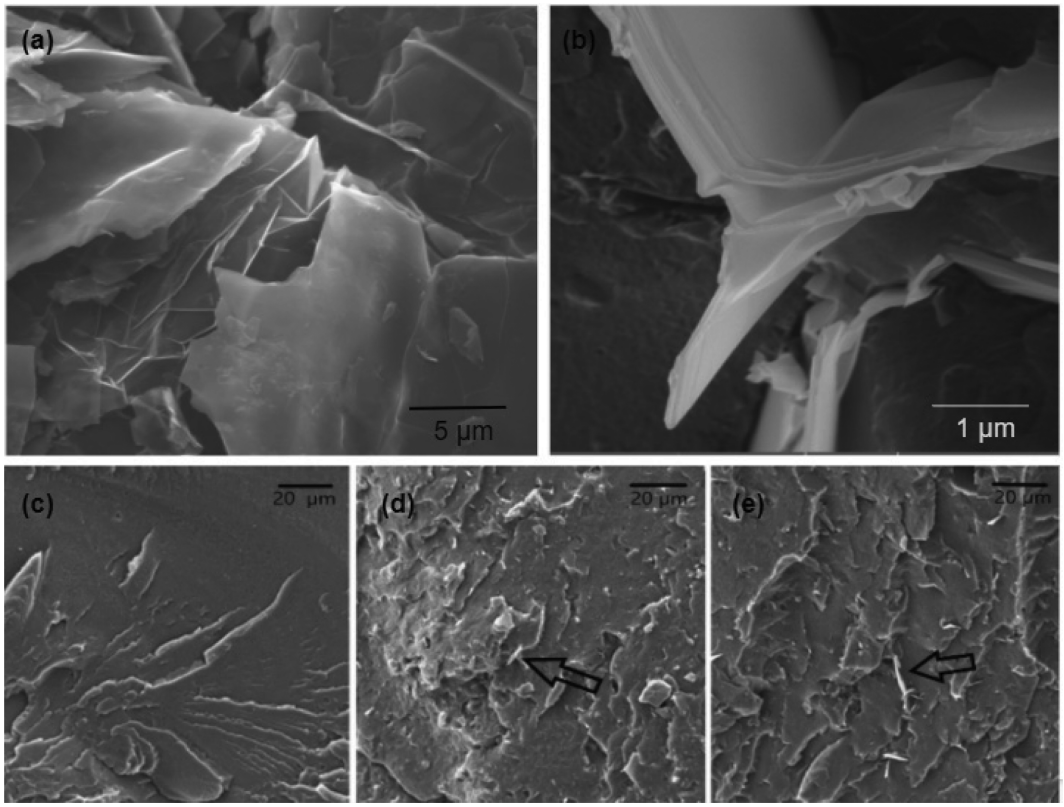

Fig. 10. Morphology of (a) GNP and (b) EPC/2GNP sample with 50 kx magnification, emphasizing the GNP layers. Surface fractured films of coatings: (c) EPC/0GNP, (d) EPC/1GNP and (e) EPC/2GNP.

[11] indicates that the process is controlled mainly by diffusion phenomena. In this case, the GNP participates in the curing reaction at early stages, leading to premature gelation and vitrification, which in turn confines interaction between the epoxy chains and functional groups of the curing agent. Therefore, the reaction will be restricted and the curing moieties get out of reach of each other. Under such a circumstance, the curing reaction is controlled by the ability of reactants to diffuse through the network, leading to a reduced degree of cure.

4. Morphology

Epoxy/GNP films were molded on Teflon plates and subsequently cryogenically fractured to analyze the influence of GNP on the fracture surface and to evaluate the morphology of the GNP when incorporated in the epoxy films. The cross-section was observed by SEM. The morphology of the GNP before incorporation and epoxy/GNP films is shown in Fig. 10.

Fig. 10(a) refers to the SEM-FEG micrograph of GNP, where its lamellar structure can be identified, with stacked layers, a wavy folded shape and to be in thin layers, typical of graphene materials. In Fig. 10(b), (c), (d) and (e), the micrographs of the fractured region of the cross-section are presented. Fig. 10(b) shows the cross section of the EPC/2GNP sample with a magnification of 50 kx with emphasis on the layered structure of the GNP. The nanosheets show edge-corrugated sheet structures which have a lateral dimension in the range of 1 µm to 3 µm, with still stacked nanosheets and some regions where few-layer structures are visible, showing some transparency.

Fig. 10(c) shows the micrograph of the EPC/0GNP sample. A relatively smooth and uniform surface is seen in the top right corner, which is typical of fragile fractures. The roughness of the surface at the bottom left could be related to the origin of the cryogenic fracture and is not related to the presence of GNP.

For samples containing GNP (Fig. 10(d) and Fig. 10(e)), surface irregularities were observed, which indicates a more ductile fracture. A similar behavior was observed by Naderi et al. [35] and by Wang et al. [18] for epoxy coatings containing graphene materials. The regions corresponding to the graphene nanoplatelets are indicated in the micrographs with arrows. Some agglomerates were formed, which was also mentioned by Zhi and Huang et al. [24] and corroborates the results so far. The presence of agglomerates may be an indication that the method used for the incorporation of GNP into solid epoxy resin was not completely effective.

CONCLUSION

The influence of the addition of GNP on the thermal properties and curing kinetics of solid epoxy resin for powder coatings was investigated. Coatings containing GNP presented a higher thermal stability in comparison to the neat epoxy. This result indicates that they can be used to improve the applicability of powder coatings in certain environments. The GNP influenced the curing behavior of the epoxy coatings by initially participating in etherification reactions, confirmed by the reduction in the activation energy, but ultimately hindering the remaining cure, as shown by the reduced

enthalpy values. The analysis based on the dimensionless CI criterion revealed that the curing state of the coatings is poor and controlled by diffusion phenomena. In general, despite the formation of agglomerates, the GNP promoted greater ductility in fractured films and higher thermal stability of the coatings.

ACKNOWLEDGEMENTS

The authors acknowledge Brazilian Agency *Coordenação de Aperfeiçoamento de Pessoal de Nível Superior* (CAPES, Brazil) - (Finance Code 001) and the *Conselho Nacional de Desenvolvimento Científico e Tecnológico* (CNPq, Brazil). The authors also thank Pulverit do Brasil for providing the components of coating formulation, University of Caxias do Sul and the *Fundação de Amparo à pesquisa do Estado do RS* (FAPERGS).

REFERENCES

1. I. Zaman, T. T. Phan, H.-C. Kuan, Q. Meng, L. T. Bao La, L. Luong, O. Youssf and J. Ma, *Polymer*, **52**, 1603 (2011).
2. International Organization for Standardization. ISO 80004-13: Graphene and related two-dimensional (2D) materials (2017).
3. J. K. Park and D. S. Kim, *Polym. Eng. Sci.*, **54**, 969 (2014).
4. B. Li and W.-H. Zhong, *J. Mater. Sci.*, **46**, 5595 (2011).
5. D. Liu, W. Zhao, S. Liu, Q. Cen and Q. Xue, *Surf. Coat. Technol.*, **286**, 354 (2016).
6. T. Kuila, S. Bose, A. K. Mishra, P. Khanra, N. H. Kim and J. H. Lee, *Prog. Mater. Sci.*, **57**, 1061 (2012).
7. M. Nonahal, H. Rastin, M. R. Saeb, M. G. Sari, M. H. Moghadam, P. Zarrintaj and B. Ramezanzadeh, *Prog. Org. Coat.*, **114**, 233 (2018).
8. L. C. Tang, Y. J. Wan, D. Yan, Y. B. Pei, L. Zhao, Y. B. Li, L. B. Wu, J. X. Jiang and G. Q. Lai, *Carbon*, **60**, 16 (2013).
9. T. K. Das and S. Prusty, *Polym-Plast. Technol.*, **52**, 319 (2013).
10. G. Gorrasi, M. Sarno, A. Di Bartolomeo, D. Sannino, P. Ciambelli and V. Vittoria, *J. Polym. Sci., Part B: Polym. Phys.*, **45**, 597 (2007).
11. M. Jouyandeh, S. M. R. Paran, A. Jannesari and M. R. Saeb, *Prog. Org. Coat.*, **127**, 429 (2019).
12. F. Ferdosian, M. Ebrahimi and A. Jannesari, *Thermochim. Acta*, **568**, 67 (2013).
13. R. Hardis, J. L. P. Jessop, F. E. Peters and M. R. Kessler, *Compos. Part A Appl. Sci. Manuf.*, **49**, 100 (2013).
14. S. Vyazovkin, K. Chrissafis, M. L. Di Lorenzo, N. Koga, M. Pijolat, B. Roduit, N. Sbirrazzuoli and J. J. Suñol, *Thermochim. Acta*, **590**, 1 (2014).
15. M. Jouyandeh, E. Yarahmadi, K. Didehban, S. Ghiyasi, S. M. R. Paran, D. Puglia, J. A. Ali, A. Jannesari, M. R. Saeb, Z. Ranjbar and M. R. Ganjali, *Prog. Org. Coat.*, **136**, 105217 (2019).
16. Y. Wang, J. Yu, W. Dai, Y. Song, D. Wang, L. Zeng and N. Jiang, *Polym. Compos.*, **36**, 556 (2015).
17. Y. Wang, J. W. Shan and G. J. Weng, *J. Appl. Phys.*, **118**, 065101 (2015).
18. F. Wang, L. T. Drzal, Y. Qin and Z. Huang, *High Perform. Polym.*, **28**, 525 (2016).
19. S. Vyazovkin, A. K. Burnham and J. M. Criado, *Thermochim. Acta*, **520**, 1 (2011).
20. L. D. Agnol, F. T. G. Dias, N. F. Nicoletti, D. Marinowic, S. Moura e Silva, A. Marcos-Fernandez, A. Falavigna and O. Bianchi, *Biomater. Appl.*, **34**(5), 673 (2019).
21. J. Opfermann, *J. Therm. Anal. Calorim.*, **60**(2), 641 (2000).
22. S. Kopsidas, G. B. Olowojoba, A. J. Kinloch and A. C. Taylor, *Int. J. Adhes. Adhes.*, **104**, 102723 (2021).
23. M. El Achaby, F. Z. Arrakhiz, S. Vaudreuil, E. M. Essassi, A. Qaiss and M. Bousmina, *J. Appl. Polym. Sci.*, **127**, 4697 (2013).
24. M. Zhi and W. Huang, *J. Wuhan Univ. Technol.*, **31**, 1155 (2016).
25. R. Mafi, S. M. Mirabedini, R. Naderi and M. M. Attar, *Corros. Sci.*, **50**, 3280 (2008).
26. U. Szeluga, S. Pusz, B. Kumanek, K. Olszowska, A. Kobyliukh and B. Trzebicka, *Crit. Rev. Solid State Mater. Sci.*, **46**, 152 (2020).
27. M. R. Acocella, C. E. Corcione, A. Giuri, M. Maggio, A. Maffezzoli and Guerra, G, *RSC Adv.*, **6**(28), 23858 (2016).
28. A. Lavoratti, A. J. Zattera and S. C. Amico, *J. Appl. Polym. Sci.*, **135**, 46724 (2018).
29. D. Romanzini, A. Frache, A. J. Zattera and S. C. J. Amico, *J. Phys. Chem. Solids*, **87**, 9 (2015).
30. A. Surnova, D. Balkaev, D. Musin, R. Amirov and A. M. Dimiev, *Composites, Part B*, **162**, 685 (2019).
31. M. G. Prolongo, C. Salom, C. Arribas, M. Sánchez-Cabezudo, R. M. Masegosa and S. G. Prolongo, *J. Therm. Anal. Calorim.*, **125**(2), 629 (2016).
32. M. Nonahal, M. R. Saeb, S. H. Jafari, H. Rastin, H. A. Khonakdar, F. Najafi and F. Simon, *Polym. Compos.*, **39**, E2016 (2018).
33. V. C. Ferrari, M. F. Azevedo, L. H. David and V. L. Lourenço, *Polímeros*, **24**(1), 123 (2014).
34. M. Erceg, I. Krešić, N. S. Vrandečić and M. Jakić, *J. Therm. Anal. Calorim.*, **131**(1), 325 (2018).
35. M. Naderi, M. Hoseinabadi, M. Najafi, S. Motahari and M. Shokri, *J. Appl. Polym. Sci.*, **135**, 46201 (2018).